Turbulent, High Schmidt Number, Entrance Region Mass Transfer in Annuli

JAMES O. CERMAK and ROBERT B. BECKMANN

University of Maryland, College Park, Maryland

Entrance region and fully developed mass transfer from the inner core of annuli was investigated for a fully developed velocity profile and a Schmidt number of 760. Constant wall concentration was the satisfied boundary condition of the inner core.

The ranges of parameters investigated were 21,400 to 75,600 for Reynolds number, 0.164 to 0.741 for the annulus diameter ratio, and 0.018 to 3.85 for the length to hydraulic diameter ratios.

Experiments were performed in an open water flow loop. Mass transfer coefficients were obtained from weight loss measurements of benzoic acid life saver elements of various diameters and lengths. These elements were assembled as an integral part of the inner core of the annulus. Concentricity was maintained by a tensioning device.

The local Sherwood number is found to be significantly affected by the annulus diameter ratio, Reynolds number, and the length to hydraulic diameter ratio. A correlation is developed which predicts 93% of the data used for its development to within ± 10%.

The design of an annular heat exchanger or a nuclear reactor requires a detailed knowledge of flow conditions, heat transfer characteristics, geometry, and overall system reaction to external forcing functions. To achieve an economic, reliable and realistic design, one must also understand the effects of system parameter variations. Annular flow literature contains numerous articles on overall behavior of heat or mass transfer systems. However, very little experimental work can be found regarding the entrance region (local variation) heat or mass transfer rates in annular systems.

Conventional correlations describe mass transfer over a relatively long length. One must have a detailed understanding of the entrance region for the design of short heat or mass transfer systems. Entrance region parameters such as Reynolds number and heat transfer length have been investigated at low Prandtl numbers (*4*, *7*). Predictions for mass transfer rate at low Schmidt numbers can be achieved by utilizing the heat to mass transfer analogy. However, there is an apparent lack of knowledge at high Schmidt numbers. There may also be an interaction between the entrance region parameters.

Another variable in the entrance region in an annulus is the diameter ratio. This effect is not well defined, although Leung, et al. (*7*) present low Prandtl number data. Usually, fully developed annulus data are correlated on the basis of hydraulic diameter and diameter ratio.

The basic objective of this paper, therefore, is to investigate entrance region mass transfer with a fully developed velocity profile at a high Schmidt number (760) and varying annulus diameter ratios. Inherent in the study is the determination of the validity of extending correlations developed for low Schmidt numbers to the high Schmidt number range. Consideration is limited to the inner core of the annulus with constant wall concentration.

The rate of mass transfer can be expressed by means of

$$N = Ak\,(C_o - C_b) \qquad (1)$$

The simplicity of the above equation is misleading, however, since k is a complicated function of the fluid flow, fluid properties, and geometry. To evaluate the mass transfer coefficient, one can measure the rate of mass transfer, the surface area, and concentrations, C_b and C_o and substitute into Equation (1).

James O. Cermak is with Westinghouse, Atomic Power Division, Pittsburgh, Pennsylvania.

The velocity distribution, for flow through a closed channel, develops from the initial condition at the inlet to a fully developed condition at some distance from the inlet. During mass transfer to a fluid, the concentration distribution is developing in an analogous manner to the velocity distribution. The initial condition in this case is the leading edge or interface of the mass transfer surface. Mass transfer rate is a function of both the velocity and concentration distributions, and therefore, a function of local position. A review of available annulus literature (*1*, *7*) reveals little experimental work regarding inner wall mass transfer as compared to the relatively large amount of heat transfer work.

Wiegand and Baker (*11*) surveyed the data on heat and mass transfer and friction in an annulus. They suggested for inner core heat transfer:

$$j = \left(\frac{h}{cG}\right)\left(\frac{c\mu}{k_t}\right)^{1-n} = K\left(\frac{D_eG}{\mu}\right)^{-0.2} \qquad (2)$$

and showed K as a graphical function of D_1/D_2 at a constant value of N_{Re}.

Later, Wiegand (*8*) recommended:

$$K = 0.023\left(\frac{D_2}{D_1}\right)^{0.45} \qquad (3)$$

Meyerink and Friedlander (*9*) investigated fully developed turbulent flow mass transfer in circular tubes. Benzoic acid, cinnamic acid, or aspirin were employed as the substance dissolving from the wall of the tube into water or aqueous solutions of sodium hydroxide. Data in the concentration entrance region was limited to three values per run, due to the size of the cylinders used. Fully developed mass transfer, for $N_{Sc} = 900$, was correlated by

$$N_{Sh} = 0.070\,N_{Re}^{0.94} \qquad (4)$$

and for $N_{Sc} = 850$ by

$$N_{Sh} = 0.168\,N_{Re}^{0.86} \qquad (5)$$

Leung, Kays, and Reynolds (*7*) studied turbulent air flow in electrically heated annuli of four different radius ratios ranging from 0.192 to 0.500. The velocity profile was fully developed upon entering the 4 ft. heated section. The ratio of heated length to hydraulic diameter varied from 23 for the 0.192 diam. ratio annulus to 73 for the 0.500 diam. ratio annulus. Data were presented in graphical form.

By the use of assumed fully developed velocity and thermal diffusivity profiles based upon literature data, the energy equation, for a fully developed temperature profile and constant heat flux, was integrated numerically. The heat transfer coefficients reported in tabular form, covered a radius ratio range from 0.10 to 1.0, an N_{Pr} range from 0 to 1,000, and an N_{Re} range from 10^4 to 10^6. Excellent agreement was obtained with the extrapolated thermal entrance length data for N_{Re} above 20,000.

Farman (4) studied inner core heat transfer to water utilizing short heated sections. The hydrodynamic entrance length was 38 equivalent diameters. Overall heat transfer coefficients were obtained and correlated by the following:

$$N_{Nu} = 0.051\,(N_{Re})^{0.78}\,(N_{Pr})^{0.4}\left(\frac{D_2}{D_1}\right)^{0.45}\left(\frac{L}{D_e}\right)^{\frac{-1.39}{N_{Re}^{0.196}}} \qquad (6)$$

EXPERIMENTAL APPARATUS

The present investigation employed a hydraulic loop, an annular test section, pressed benzoic acid elements, taps for pressure drop determination, and associated instrumentation.

This hydraulic loop consisted of a pump, 1½-in. type L streamline copper tubing and galvanized pipe, and a holdup tank, open to the atmosphere. The water flowed from the holdup tank to the centrifugal pump, then to the test section and returned to the holdup tank. The inlet and outlet flow connections of the test section are situated at an angle of 90 deg. to the test section following the usual pattern of annulus construction.

Annular Test Section

Four different annulus geometries were studied, the dimensions and diameter ratios being given in Table 1. In all cases copper tubing was utilized for the inner core and outer wall of the annulus, except for the inner core diameter of ¼ in. In this particular case a steel rod was used.

These test sections were constructed to enable axial movement. Concentricity was maintained by end fittings and tensioning (See Figure 1). The length of the outer tube of the annulus was varied. This maintained the same hydrodynamic entrance length for each test section. [The (¼) test section was shorter as can be seen from Table 1].

TABLE 1. ANNULUS DIMENSIONS

Test section designation	Annulus Dimensions: I.D. of outer wall D_2, in.	Annulus Dimensions: O.D. of inner core D_1, in.	D_1/D_2	Hydrodynamic entrance length L/D_e	Hydrodynamic exit length L/D_e
(1/4)	1.520	0.250	0.164	62	34
(1/2)	1.520	0.500	0.329	76	41
(7/8)	1.520	0.875	0.576	76	41
(9/8)	1.520	1.125	0.740	76	41

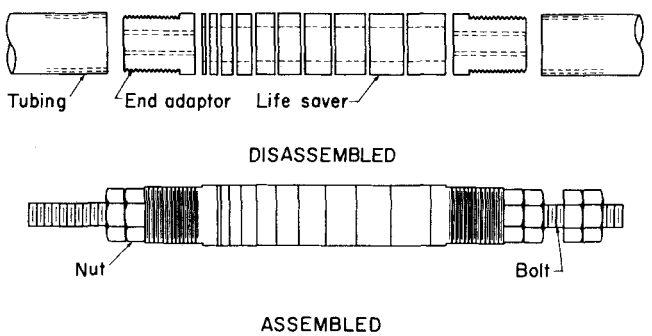

Fig. 1. The annular text section.

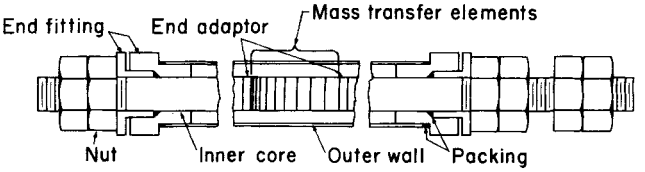

Fig. 2. The mass transfer section.

Mass Transfer Section

Mass transfer coefficients were determined from the rate of dissolution of benzoic acid from the inner core of the annulus. The pressed benzoic acid elements resembled life savers.

The inner core for the (½), (7/8), and (9/8) test sections consisted of (moxing axially along the inner core) a length of tubing, end adaptor, life savers, end adaptor, and length of tubing (see Figure 2). Mass was transferred from the outside diameter of the life saver, with from 7 to 14 life savers stacked together during each run. Life savers were manufactured in molds(1) made by the authors. The compression pressure was 15,000 lb./sq. in.

Life savers had a smooth, hard finish, sharp edges, and were brittle. No attempt was made to measure the weight of benzoic acid added to the mold. It was more accurate to weigh the finished life saver and measure its thickness with a micrometer. Life savers varying more than 0.001 in. in thickness across the face were discarded.

A different design was employed for the (¼) test section. The inner core of this test section consisted of a long steel rod with a 1 in. long notch. The mass transfer elements were benzoic acid shaped to fit the notch. They were held in place by rubber fillers, inserted downstream of the mass transfer elements.

EXPERIMENTAL PROCEDURE

The experimental procedure involved inserting life savers as an integral part of the inner core of the annulus, flowing water through the annulus for a predetermined length of time, and determining the mass transfer coefficient from the amount of weight lost by the individual mass transfer elements.

The experiment was designed with three replicates to investigate the effects of the diameter ratio (the ratio of the outer diameter of the annulus to the inner diameter of the concentric tube), the mass transfer length, and the Reynolds number. The program consisted of a total of 72 runs covering the following nominal values of the parameters:

N_{Re}: 21,400; 33,200; 55,500; 75,600

D_1/D_2: 0.164, 0.329, 0.576, 0.740

In addition, each run yielded from 7 to 14 data points with the length of the mass transfer elements as the parameter. Water temperature was maintained constant at 30°C, within 0.2°C., throughout the entire test program.

Pressure drop data were obtained for all four test sections without the mass transfer section, prior to initiation of mass transfer runs. These data were taken primarily to demonstrate that the apparatus was conventional. No unusual effects were noted.

Initially, several preliminary tests were performed to determine the allowable time duration for each of the runs. It was decided to limit the change in diameter of the inner core to 4% or less. Since the rate of mass transfer is greatest for the first mass transfer element, this element determines the time duration of the run. Runs were performed in the range of 1 to 4% change in diameter and as illustrated by Figure 3 demonstrate no effect, within the experimental accuracy of the data, as a function of the time duration of the run. In an effort to achieve greater accuracy for the (¼) test section (very small differences in weight were measured), diameter changes as high as 6.5% were permitted.

Another object of continual investigation throughout the study related to the possibility of an interfacial or edge effect of the mass transfer element. By the insertion of varying thicknesses of the mass transfer element, in the region of fully

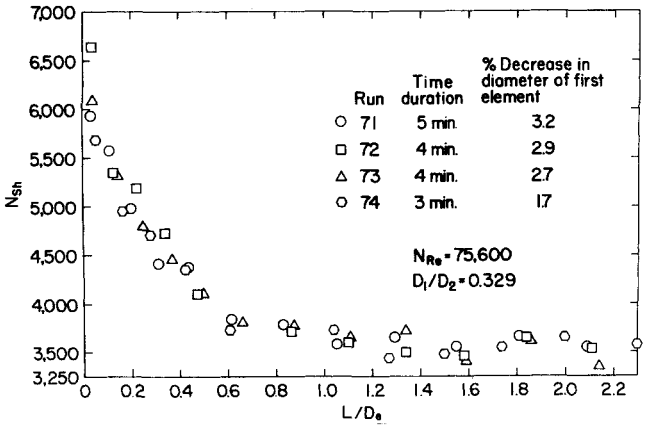

Fig. 3. The effect of the run duration time on the Sherwood number.

developed mass transfer, it was determined that no interfacial or edge effect existed within the experimental accuracy of the data. In addition, the element thickness was checked after several runs and was found to be identical to the original thickness.

Inner core location in the annulus was studied by positioning the mass transfer elements 5 in. upstream of the normal location. Since the experimental results were within the experimental accuracy of the data, no discernible effect could be noted. From the pressure drop data it is believed that, at 75 diam., one is very close to or at fully developed flow conditions.

Correction for the change in concentration of the main stream was neglected, because of the large water volume in the system and the relatively small amount of benzoic acid dissolved during a run. In addition, the water was changed after every three runs.

Drainage of water from the test section was accomplished in approximately 15 sec. During this period the inner core was covered with water only part of the time. This effect was found to be quite small, as evaluated by comparison to preliminary runs of elements immersed in static water for similar time periods, and was neglected.

The surface of the elements in general were smooth in appearance and to the touch both before and after a run. Occasionally the elements were pitted or became chipped in handling. All data involving chipped or broken elements were discarded. If the inner core was not mounted properly, as determined by probing the concentricity of the inner core before and after each run, the entire run was discarded.

RESULTS

Fully Developed Mass Transfer

Initially, all of the data were examined to determine the approximate axial location where the onset of fully developed mass transfer occurs. This length to achieve fully developed mass transfer varied with Reynolds number and test section. Only data from the (1/2), (7/8), and (9/8) test sections could be utilized in the establishment of a correlation, since fully developed mass transfer conditions were not achieved for the (1/4) test section. In addition, the scatter of the data for the (1/4) test section was such that even if fully developed mass transfer were achieved, it would be virtually impossible to determine the approximate point of initiation. Data in this fully developed region were used to determine the Reynolds number and diameter ratio effect on the Sherwood number.

Results shown in Figure 4 demonstrate a linear relationship between Sherwood number and Reynolds number, expressed in logarithmic coordinates, for each test section. This Reynolds number effect can be correlated by:

$$(N_{Sh})_D = f\left(\frac{D_2}{D_1}\right)(N_{Re})^{0.91} \qquad (7)$$

There may be a Reynolds number-diameter ratio interaction on the Reynolds number exponent. It was felt, however, the accuracy of the data did not justify the establishment of this effect.

The diameter ratio effect was determined by plotting $(N_{Sh})_D/(N_{Re})^{0.91}$ as a function of D_2/D_1. This resulted in a fully developed mass transfer correlation expressed by:

$$(N_{Sh})_D = 0.093\,(N_{Re})^{0.91}\left(\frac{D_2}{D_1}\right)^{0.30} \qquad (8)$$

Since all data were obtained at only one Schmidt number (760), no Schmidt number effect can be deduced from the data. Rather than introduce a typical literature effect of Schmidt number into the equation, for example, $(N_{Sc})^{1/3}$, an exact representation of the data was thought to be preferable.

Entrance Region Mass Transfer

All of the data, except for the (1/4) test section (for the reasons given previously) were plotted as the ratio of local to fully developed Sherwood number as a function of the length to hydraulic diameter ratio. The fully developed Sherwood number was defined by Equation (8). Figures 5 and 6 yield an insight into the diameter ratio and Reynolds number dependence of the data. The data points have been omitted for clarity.

Figure 5 demonstrates, for a given N_{Re}, that the entrance region length (as expressed by length to hydraulic diameter ratio) decreases as D_2/D_1 increases. Also for a given L/D_e and N_{Re}, $(N_{Sh})_L/(N_{Sh})_D$ decreases as D_2/D_1 increases. In Figure 6, for a given diameter ratio, the entrance region length decreases as N_{Re} increases. For a given L/D_e and D_2/D_1, $(N_{Sh})_L/(N_{Sh})_D$ decreases as N_{Re} increases. All of the data exhibited the above patterns of behavior.

It was found that the following equational form:

$$\frac{(N_{Sh})_L}{(N_{Sh})_D} = 1 + a\,e^{-b\left(\frac{L}{D_e}\right)} \qquad (9)$$

represented the data well. This form, also allows correlation of entrance and fully developed region data in one

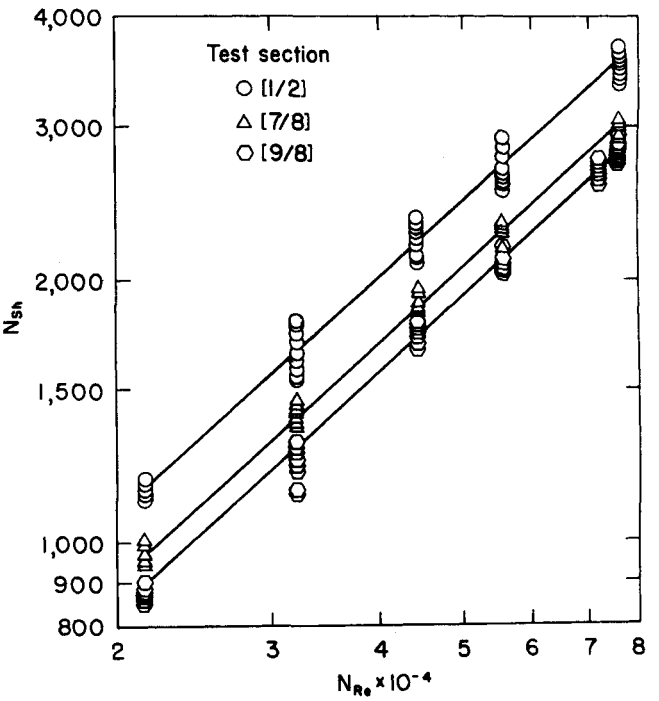

Fig. 4. The effect of the Reynolds number on the fully developed Sherwood number.

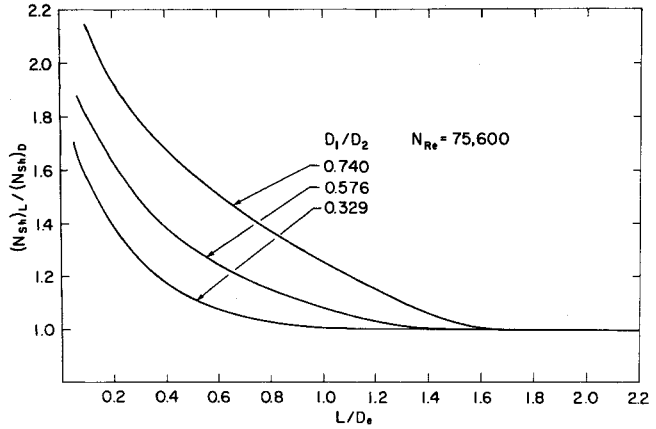

Fig. 5. Entry region behavior as a function of annulus diameter ratio.

equation. The only shortcoming is that the exponential does not die as fast as the data. The magnitude of the deviation is small, but the predicted entrance length to reach, for example, a $(N_{Sh})_L/(N_{Sh})_D = 1.01$, is long in comparison to the data.

Evaluation of a and b yielded the following:

$$a = 17.9\, N_{Re}^{-0.326}\, e^{1.4\left(\frac{D_1}{D_2}\right)} \qquad (10)$$

and

$$b = 0.05\, N_{Re}^{0.4}\left[1 - 0.265\, N_{Re}^{0.1}\left(\frac{D_1}{D_2}\right)\right] \qquad (11)$$

Setting $z = (N_{Sh})_L/(N_{Sh})_D$ and multiplying Equation (8) by $(N_{Sh})_L/(N_{Sh})_D$ gives

$$(N_{Sh})_L = 0.093\, (N_{Re})^{0.91}\left(\frac{D_2}{D_1}\right)^{0.30} z \qquad (12)$$

It should be recognized that equation (12) has the limitation that:

$$1 - 0.265\, N_{Re}^{0.1}\left(\frac{D_1}{D_2}\right) > 0$$

or

$$N_{Re}^{0.1}\left(\frac{D_1}{D_2}\right) < 3.78$$

This limitation is satisfied for the range of variables investigated in this study.

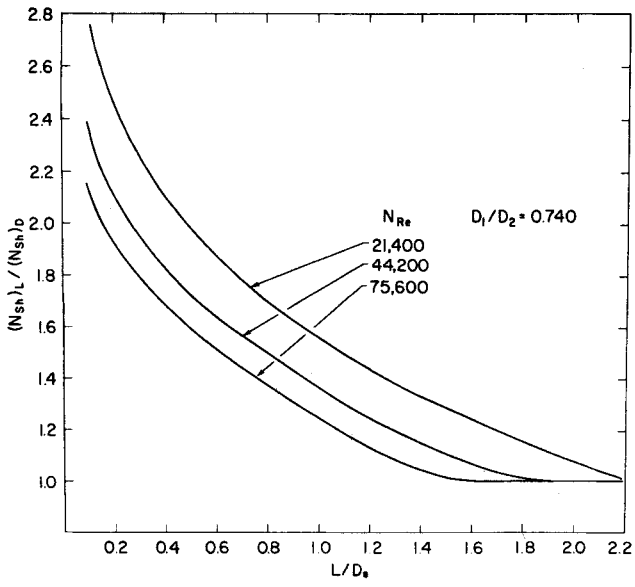

Fig. 6. Entry region behavior as a function of Reynolds number.

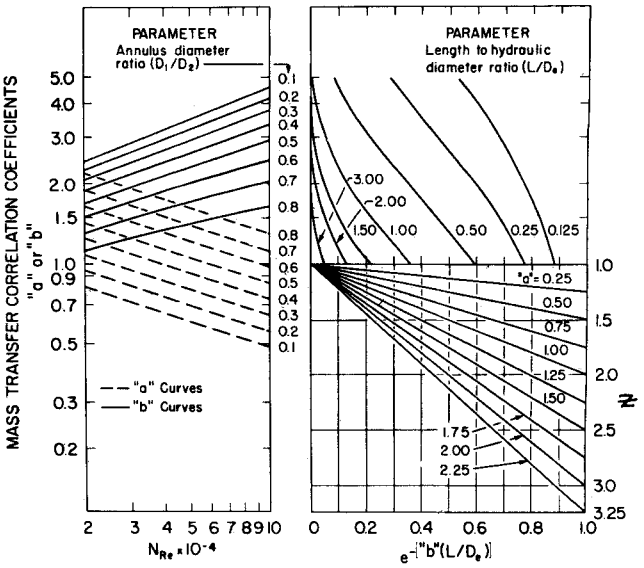

Fig. 7. Graphical solution of entry region mass transfer correlation.

To facilitate evaluation of the above equation, a graphical technique, as shown in Figure 7, was employed to evaluate z. The following procedure is used with N_{Re}, D_1/D_2, and L/D_e given:

1. N_{Re} and D_1/D_2 define a in the left graph
2. N_{Re} and D_1/D_2 define b in the left graph
3. b and L/D_e define $e^{-b(L/D_e)}$ in the upper right graph
4. a and $e^{-b(L/D_e)}$ define z in the lower right graph

All of the data, except the (1/4) test section, have been graphed in Figure 8 as $(N_{Sh})_{L\text{-meas.}}$ vs. $(N_{Sh})_{L\text{-calc.}}$ The (1/4) test section data are shown in Figure 9 as compared to the correlation. There are 785 data of which 167 are for the (1/4) test section. Good agreement was obtained for the (1/2), 7/8), and (9/8) test sections. Based on counting data, 93% of these data fall within ±10% of the correlation. Maximum deviation from the correlation for these data was 22%. The (1/4) test section data showed poor agreement with the correlation. This was expected because they were not used to develop the correlation and they were highly scattered. Of these data, 78% fall within +10 and −20% of the correlation. Maximum deviation from the correlation was 33%.

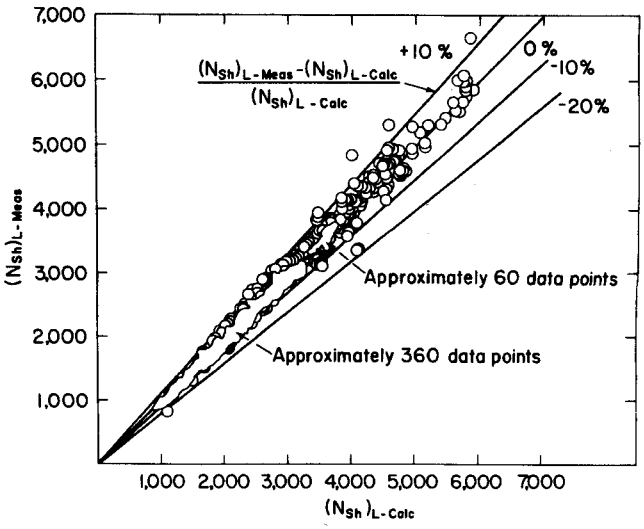

Fig. 8. Comparison of the proposed correlation equation with the (1/2), (7/8), and (9/8) test section data.

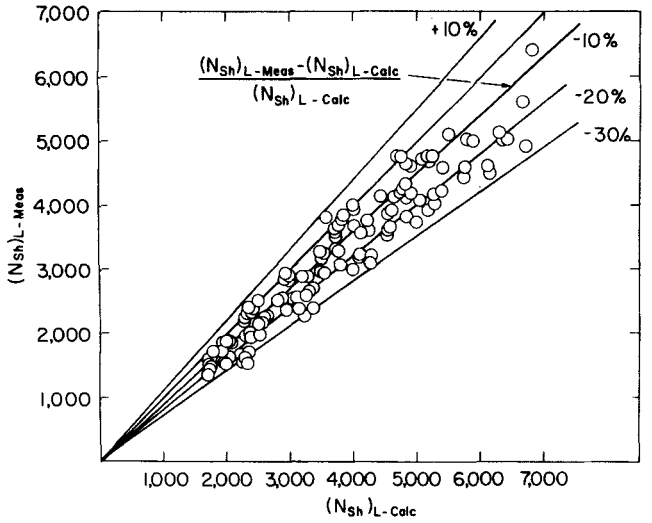

Fig. 9. Comparison of the proposed correlation equation with the (1/4) test section data.

DISCUSSION

Fully Developed Mass Transfer

The results for this region are discussed in relation to existing correlations and the analytical models proposed by Leung, Kays, and Reynolds (7) and Deissler (2). Valid comparisons are limited, however, due to the lack of previous experimental work in the high Schmidt number range. In addition, both of the analytical models above are for uniform heat or mass flux, whereas this study was performed under constant wall concentration conditions. This inconsistency in comparison is believed to be of small consequence, because Deissler (3) compared analytical results for constant wall temperature and uniform heat flux and found negligible differences at a Prandtl number of 0.73.

The Reynolds number dependency, $N_{Re}^{0.91}$, agrees fairly well with high Schmidt number results for circular tubes. Meyerink and Friedlander (9) found a N_{Re} dependency of $N_{Re}^{0.94}$ and $N_{Re}^{0.86}$ for N_{Sc} of 900 and 850, respectively, using benzoic acid and aspirin in circular tubes. Harriott and Hamilton (6) have found, for circular tubes, a dependency of $N_{Re}^{0.913}$ for a Schmidt number range of 430 to 10,000. This dependency is not, however, consistent with Wiegand (11) ($N_{Re}^{0.8}$), Farman (4) ($N_{Re}^{0.8}$), Monrad and Pelton (10) ($N_{Re}^{0.8}$), and many other investigators in the low Prandtl number range.

The diameter ratio dependency, $(D_2/D_1)^{0.30}$ does not agree with Wiegand $(D_2/D_1)^{0.45}$ or Monrad and Pelton $(D_2/D_1)^{0.53}$. This difference in diameter ratio effect could result from a Schmidt number effect.

The comparison of Equation (8) to other experimental correlations is shown in Figure 10. Only one diameter ratio ($D_2/D_1 = 2.0$) is considered for clarity. In addition the correlations have been graphed as if they were mass transfer results instead of heat transfer. Comparison shows that the analysis of Leung, et al. is 28 to 32% lower than the present correlation. Their slope of N_{Sh} as a function of N_{Re} is very similar to the present correlation. Other correlations are from 5% higher to 35% lower, except for the Foust and Christian correlation which is from 230 to 270% higher. It should be noted that fairly good agreement was obtained with the Farman correlation. Admittedly, the N_{Re} and D_2/D_1 dependence are different from Farman's correlation, but the N_{Sh} calculated from his heat transfer correlation is the closest to the present correlation in absolute magnitude. The Leung, et al. analysis is lowest in absolute magnitude of all works shown except for the cross-over of the Monrad and Pelton correlation.

Entrance Region Mass Transfer

Effects in the entrance region should be governed entirely by the variation in parameters at or very close to the wall at high Schmidt numbers. This results because the concentration profile is very steep at the wall and quite flat in the main stream. The analysis of circular tubes by Deissler (2) supports the above statement at high Schmidt numbers. Experimental results in the annular entrance region are limited to heat transfer studies by Farman (4) ($N_{Pr} = 5.6$) and Leung, et al. (7) ($N_{Pr} = 0.70$). Analytical studies of the annular entrance region have not been performed to our knowledge.

The results of the present study indicate effects of diameter ratio, length to hydraulic diameter ratio, Reynolds number, and a diameter ratio (Reynolds number interaction in the entry region). In general, Deissler (2) showed for circular tubes the entrance length (as reprented by L/D) decreases as N_{Sc} increases until at very high N_{Sc}, the trend is reversed. Increasing N_{Re} decreases the entrance length except at low N_{Sc}, where again the trend is reversed. There is no diameter effect when entrance length is expressed as L/D, because the dimensionless parameters are independent of diameter for a constant N_{Re}. For example:

$$r_o^+ = \frac{r\sqrt{\frac{\tau_w}{\rho_w}}}{\frac{\mu_w}{\rho_w}}, \quad r = \frac{D}{2}$$

and for a constant N_{Re}:

$$\tau_w = \frac{K}{D^2}$$

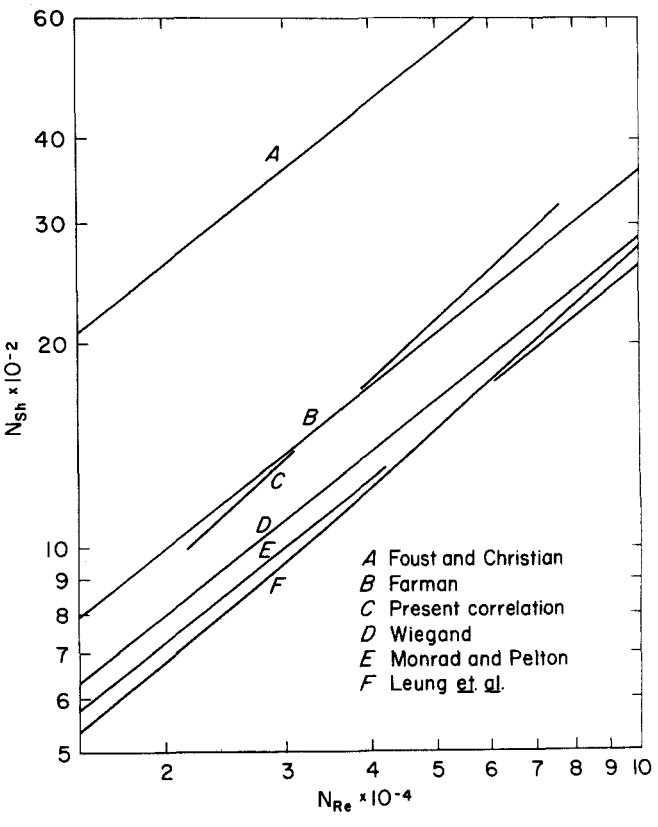

Fig. 10. Comparison of fully developed mass transfer correlations for a diameter ratio, D_2/D_1, of 2.0 and a Schmidt number of 760.

and

$$r_o^+ = \frac{D}{2}\frac{\sqrt{\frac{K}{D^2\rho_w}}}{\frac{\mu_w}{\rho_w}} = \frac{1}{2}\frac{\sqrt{\frac{K}{\rho_w}}}{\frac{\mu_w}{\rho_w}}$$

where K is a constant.

For a constant high N_{Sc}, as N_{Re} increases r_o^+ increases, thus, reducing the entrance length. Comparison of entrance region experimental results for circular tubes to Deissler's analysis yield the same N_{Re} effect, but $(N_{Sh})_L(N_{Sh})_D$ data values are generally higher than the analytical results for the same N_{Sc}, L/D, and N_{Re}.

The entrance region in this study demonstrates a D_1/D_2 effect on L/D_e for a constant N_{Re}. It is believed that this effect can be explained by the inner wall shear stress, which can be expressed by:

$$\tau_1 = K^2\frac{f\left(\frac{D_2}{D_1}\right)}{D_e^2}$$

(K is a constant for a given N_{Re}) and is not just proportional to $1/D^2$ as discussed above for circular tubes. The definition of $f(D_2/D_1)$ is unknown because of the lack of knowledge regarding the radius of maximum velocity. An estimate of τ from laminar flow theory shows that as D_1/D_2 decreases, $D_e\sqrt{\tau_1}$ increases. Therefore, L/D_e should decrease as D_1/D_2 decreases, for a given N_{Re}. This effect is consistent with the entrance region data obtained in this study.

Leung, et. al. obtained entrance region heat transfer data at $N_{Pr} = 0.70$ and D_1/D_2 ranging from 0.192 to 0.500. The data are presented in Figure 11, and it is noticed that a diameter ratio effect on L/D_e exists for a N_{Re} of approximately 40,000. This diameter ratio effect was apparent for the complete range of N_{Re} studied.

For a given N_{Re} and L/D_e, $(N_{Nu})_L/(N_{Nu})_D$ increases as D_1/D_2 increases. The entrance length to reach fully developed flow extends beyond the range of the data, and because the data are very closely grouped at $L/D_e > 30$, it is difficult to determine if any D_1/D_2 effect exists on the entrance length. The D_1/D_2 effect established by this data is consistent with the present study.

Another effect of the present study is that L/D_e decreases as N_{Re} increases. This can also be explained by the $D_e\sqrt{\tau_1}$ term. As N_{Re} increases, τ_1 increases and, thus, entrance length decreases. This is the same effect that was demonstrated in Deissler's analytical development of circular tubes and is consistent with Farman's work. This investigation also produced a N_{Re}-D_1/D_2 interaction effect on $(N_{Sh})_L/(N_{Sh})_D$. A possible explanation is that the radius of maximum velocity is a function of N_{Re}. Thus, $f(D_1/D_2)$ defined previously would be N_{Re} dependent.

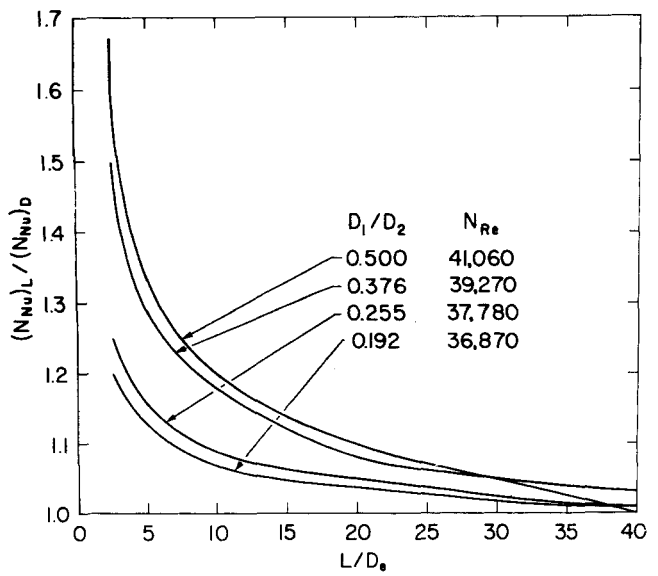

Fig. 11. Ratio of local Nusselt number to the fully developed Nusselt number for a Prandtl number of 0.70.

SUMMARY

A summary of the findings of this investigation are as follows:

1. An equation was developed that correlated entrance region and fully developed mass transfer in annuli at a Schmidt number of 760.
2. Entrance region mass transfer was found to be dependent on diameter ratio of the annulus, Reynolds number, and length to hydraulic diameter ratio.

NOTATION

A = surface area, sq.ft.
C = concentration of diffusing substance
C_b = bulk concentration of diffusing substance
c = specific heat of fluid, (B.t.u.)/[(lb.m)(°F.)]
D = inside diameter of circular tube, ft.
D_1 = outside diameter of inner core of annulus, ft.
D_2 = inside diameter of outer tube of annulus, ft.
D_e = hydraulic diameter for annulus, $(D_2 - D_1)$ ft.
G = mass velocity, ρV, (lb.$_m$)/[(sec.)(sq.ft.)]
h = heat transfer coefficient, (B.t.u.)/[(sec.)(sq.ft.)(°F.)]
j = Colburn j factor
k = mass transfer coefficient, ft./sec.
k_t = thermal conductivity, (B.t.u.)/[(sec.)(ft.)(°F.)]
L = length of mass transfer surface, ft.
N = rate of mass transfer toward tube center, lb.$_m$/sec.
N_{Nu} = Nusselt number, $(h D/k_t)$ or $(h D_e/k_t)$
$(N_{Nu})_L$ = local Nusselt number
$(N_{Nu})_D$ = fully developed Nusselt number
N_{Pr} = Prandtl number, $(C_p\mu/k_t)$
N_{Re} = Reynolds number, $(\rho V D/\mu)$ or $(\rho V D_e/\mu)$
N_{Sc} = Schmidt number, $(\mu/\rho\lambda)$
N_{Sh} = Sherwood number, (kD/λ) or (kD_e/λ)
$(N_{Sh})_L$ = local Sherwood number
$(N_{Sh})_D$ = fully developed Sherwood number
r_o = radius of circular tube, ft.
r_1 = outside radius of inner core of annulus, ft.
r_2 = inside radius of outer tube of annulus, ft.
r_o^+ = circular tube radius parameter, $(\sqrt{\tau_o/\rho_o}/\mu_o/\rho_o)r_o$

Greek Letters

λ = diffusion coefficient, sq.ft./sec.
μ = fluid viscosity, (lb.$_m$)/[(ft.)(sec.)] or [(lb.$_f$)(sec.)]/(sq.ft.)
ν = kinematic viscosity, sq.ft./sec.
ρ = mass density of fluid, lb.$_m$/cu.ft.
τ = shear stress, lb.$_f$/sq.ft.

Subscripts

o = wall
1 = inner wall
2 = outer wall

LITERATURE CITED

1. Cermak, J. O., Ph.D. thesis, Univ. Maryland, (1966).
2. Deissler, R. G., *Nat. Advisory Comm. Aeron., Rep. 1210* (1955).

3. *Ibid., Tech. Note 3016* (1953).
4. Farman, R. F., Symposium on Fundamentals of Heat and Mass Transfer, preprint 48A (1965).
5. Foust, A. S., and G. A. Christain, *Trans. Am. Soc. Mech. Eng.*, **36**, 541 (1940).
6. Harriott, P., and R. M. Hamilton, *Chem. Eng. Sci.*, **20**, 1073 (1965).
7. Leung, E. Y., W. M. Kays, and W. C. Reynolds, *Rept AHT-4*, Stanford Univ., California (1962).
8. McMillen, E. L., and R. E. Larson, *Trans. AIChE*, **41**, 147 (1945).
9. Meyerink, E. S. C., and S. K. Friedlander, *Chem. Eng. Sci.*, **17**, 121 (1962).
10. Monrad, C. C., and J. F. Pelton, *Trans. AIChE*, **38**, 593 (1942).
11. Weigand, J. H., and E. M. Baker, *ibid.*

Manuscript received September 7, 1967; revision received January 21, 1968; paper accepted January 24, 1968.

Joule-Thomson Effects in Gas Mixtures: The Nitrogen-Methane-Ethane System

R. C. AHLERT and L. A. WENZEL

Lehigh University, Bethlehem, Pennsylvania

Pressure-temperature data were obtained along isenthalps for nitrogen, methane, and three ternary nitrogen-methane-ethane mixtures. These data were differentiated to obtain Joule-Thomson coefficients over the temperature range from ambient to 200°K. and at pressures from 165 atm. to about 5 atm. Data for nitrogen was obtained down to 140°K.

The resulting Joule-Thomson coefficients were compared with predictions based on the Beattie-Bridgeman and Benedict-Webb-Rubin equations of state and on the virial equation of state truncated after the third virial coefficient. These comparisons show that the Benedict-Webb-Rubin equation could predict the data with a deviation averaging 1.7%. The Beattie-Bridgeman predictions were highly dependent upon the mixture rules used, with the best set of mixture rules giving an absolute average deviation of 4.8%. Predictions using the virial equation with virial constants obtained from the Lennard-Jones potential energy function using a geometric mean minimum potential energy deviated from the experimental data by 5%.

In all of these comparisons, the virial coefficients of ethane appear to be in greatest uncertainty, and the predictions of mixture data high in ethane were least satisfactory. Thus it appears that improved data on the pure components, particularly ethane, are vital to any satisfactory evaluation of mixture properties.

Most methods for treating the thermodynamic properties of gas mixtures make a basic assumption that equations of state for mixtures have the same form as the equations that describe the component species. Constants for mixture relations are obtained by a combination of the constants of the components. Many empirical rules have been proposed as means of making these combinations. This research was concerned with a comparison and evaluation of a number of such mixing rules. First, effort was directed toward developing a body of accurate data for ternary gas mixtures, over a useful range of pressures, temperatures, and compositions. Second, these data were used to test the ability of mixing rules for empirical and virial equations of state to predict properties for multicomponent mixtures. Third, the experimental mixtures were observed under conditions at which one of the component species was condensable in its pure state; these data were used to examine the extrapolation of equation-of-state parameters for the condensable species.

Three mixtures of ethane, methane, and nitrogen were investigated. Experiments consisted of measuring Joule-Thomson effects across an insulated throttling valve. The apparatus is suited to operation at temperatures from −200 to 25°C. and pressures to 165 atm. A three-fold variation in ethane concentration was chosen and experiments spanned a broad region in which this component is condensed when pure. The Beattie-Bridgeman, Benedict-Webb-Rubin, and virial equations were the basis for examination of mixing rules.

R. C. Ahlert is at Rutgers University, New Brunswick, New Jersey.